



# Integrated valorization of *Moringa oleifera* and waste *Phoenix dactylifera* L. dates as potential feedstocks for biofuels production from Algerian Sahara: An experimental perspective



A. Boulal<sup>a,b</sup>, A.E. Atabani<sup>c,\*</sup>, M.N. Mohammed<sup>d</sup>, M. Khelafi<sup>a</sup>, Gediz Uguz<sup>e</sup>, Sutha Shobana<sup>f</sup>, Awais Bokhari<sup>g</sup>, Gopalakrishnan Kumar<sup>h</sup>

<sup>a</sup> Unité de Recherche en Energie Renouvelables en Milieu Saharien, URERMS, Centre de Développement des Energies Renouvelables, CDER, 01000, Adrar, Algeria

<sup>b</sup> Laboratoire des Ressources Naturelles Sahariennes, Université Ahmed Draya, Arar, Algeria

<sup>c</sup> Green Processing, Bioremediation and Alternative Energies Research Group, Faculty of Environment and Labour Safety, Ton Duc Thang University, Ho Chi Minh City, Vietnam

<sup>d</sup> Alternative Fuels Research Laboratory (AFRL), Energy Division, Department of Mechanical Engineering, Faculty of Engineering, Erciyes University, Kayseri, 38039, Turkey

<sup>e</sup> Department of Chemical Engineering, Ondokuz Mayıs University, 55200, Samsun, Turkey

<sup>f</sup> Department of Chemistry and Research Centre, Aditanar College of Arts and Science, Tamil Nadu, India

<sup>g</sup> Department of Chemical Engineering, COMSATS University Islamabad (CUI), Lahore Campus, Defense Road Off Rawind Road, Lahore, Pakistan

<sup>h</sup> Institute of Chemistry, Bioscience and Environmental Engineering, Faculty of Science and Technology, University of Stavanger, Box 8600 Forus, 4036, Stavanger, Norway

## ARTICLE INFO

### Keywords:

*Moringa oleifera* seeds  
Waste *Phoenix dactylifera* L. dates  
Waste valorization  
Biodiesel  
Bioethanol  
Characterization

## ABSTRACT

The world is concerned with the degradation of the Saharan eco-system due to the absence of green spaces, emission of greenhouse gases and the burial of oases by sand beside the global energy crisis. This promoted the Algerian government to set a national strategy towards the use of renewable sources to cover 40% of its energy needs by 2030. In this article, a modern technique to simultaneously protect the environment and produce biofuels from the Saharan environment through cultivation of *Moringa oleifera* and valorizations of waste *Phoenix dactylifera* L. dates which are of not of satisfactory quality for the local market has been adopted. Characterization of *Moringa oleifera* oil, *Moringa oleifera* biodiesel and bioethanol produced from the waste date was done. Biodiesel-diesel-bioethanol blends were characterized by DSC, FT-IR, TGA and GC methods. Results show high oil content of *Moringa oleifera* seeds of 40%, biodiesel yield of 91% and bioethanol percentage of 96.83% with 3.17% of impurities. The properties of ternary blends of D80B5BE15, D80B10BE10 and D80B15BE5 exhibit similar densities and cold flow properties to Euro-diesel. Our analysis also proved that waste *Phoenix dactylifera* L. dates are useless as ruminant feed due to low protein content. In conclusion, the study proved the feasibility of cultivating *Moringa oleifera* to protect the environment and valorizing its seeds besides waste date seeds to produce both biodiesel and bioethanol in the Algerian Saharan.

## 1. Introduction

The fossil-based energy demand is rapidly increasing in a daily basis around the globe, which would be not beneficial for human ecology. Moreover, fossil-based resources are not renewable and their consumption with the current rhythm will lead to the disappearance of the reserves in a few decades. Global warming issue caused by burning fossil fuel pushes the world to produce renewable and environmental friendly fuel from sustainable feedstock (Sarvanan et al., 2018). Thus, biofuels production such as biodiesel, biohydrogen, biogas and

bioethanol (BE) from waste (Prabakar et al., 2018; Atabani et al., 2019a, 2019b) has been much considered recently. Biodiesel, being one of these promising options, is an alternative and renewable diesel fuel, which exhibits similarity with the fossil diesel. Combustion of biodiesel produces less serious emissions compared to fossil diesel (Atabani et al., 2012, 2013a, 2013b). Moreover, BE has also been considered as a viable alternative fuel to both the petrol and diesel engines (Nanthagopa et al., 2017). BE can be produced through alcoholic fermentation of sugar from vegetable materials and agricultural residues (Keskin et al., 2013). Recently, blending BE with diesel and biodiesel in (CI)

\* Corresponding author.

E-mail address: [abdulaziz.atabani@tdtu.edu.vn](mailto:abdulaziz.atabani@tdtu.edu.vn) (A.E. Atabani).

<https://doi.org/10.1016/j.bcab.2019.101234>

Received 2 June 2019; Received in revised form 30 June 2019; Accepted 3 July 2019

Available online 04 July 2019

1878-8181/ © 2019 Published by Elsevier Ltd.

### Nomenclature

ADL	Acid detergent lignin
AOCS	American Oil Chemists' Society
BE/BE100	Bioethanol
CF	Crude fiber
CFPP	Cold filter plugging point
CIME	<i>Calophyllum inophyllum</i> methyl ester
CMOO	Crude <i>Moringa oleifera</i> oil
CP	Cloud point
D/D100	Euro diesel
DE	Determination of elements
DF	Determination of FAT
DM	Dry matter
DSC	Differential scanning calorimetry

FAC	Fatty acid composition
FT-IR	Fourier transform infrared spectroscopy
GC	Gas chromatography
MO	<i>Moringa oleifera</i>
MOME/B100	<i>Moringa oleifera</i> methyl ester (biodiesel)
PP	Pour point
SCGO	Spent coffee grounds oil
SCP	Soluble crude protein
TAC	Total ash content
TGA	Thermogravimetric analysis
WCOME/SCGOME	Waste cooking/spent coffee grounds oils methyl ester
WCO/SCGO	Mix of waste cooking and spent coffee grounds oils (50/50% volume)
WD	Waste <i>Phoenix dactylifera</i> L. dates

Compression Ignition engines has become an important area of research (Keskin et al., 2013; Labeckas et al., 2014; Nanthagopal et al., 2017). Addition of BE in CI engines can significantly reduce the particulate matter (PM) emissions (Keskin et al., 2013), thereby utilization of such fuels marks a change towards sustainable energy.

The Algerian government developed a national program for the years 2011–2030 that set concrete actions to promote energy efficiency, renewable energies and to reduce the dependence on fossil fuels as well as a production of alternative fuels. This research article proposed to implant *Moringa oleifera* (MO) tree in the State of Adrar (Fig. 1), Algerian Saharan due to its fast growth and its adaptation to the Saharan climate, it's fertilizing effect on the poor grounds on the nutrients and its fruits which are produced after one year of setting-up. The tree also acts as a protector to the environment and as a solution for the degradation of the Saharan ecosystem and burial of oases by sand in Algeria besides, its use for food and other beneficial applications (Premi et al., 2010). This plant is the most widely cultivated species from the genus *Moringa* which belongs to the family *Moringa cease* (Hsu et al., 2006).

Fig. 2 shows some photographs of MO tree and seeds planted in Adrar state. The seeds have excellent oil content. The high percentage of oleic acid in crude *Moringa oleifera* oil (CMOO) (70–75%) makes it

suitable for soap making and industrial uses such as fine lubricant and perfumery (Machell, 1994; Lalas and Tsaknis, 2002; Mohammed et al., 2003; Anwar et al., 2006). *Moringa* seed oil is also popular supplement in many countries for its exceptional nutritional and health benefits (Ruttarattanamongkol et al., 2014). The oil yield from the seeds depends on the nature of the solvent, the temperature of extraction, seed particle size, contact (residence) time between the solvent and the seed and pre-treatment conditions (Sayyar et al., 2009). Another advantage of *Moringa* oil is its good potential for producing biodiesel (Mofijur et al., 2014a, 2014b).

On the other hand, the date palm potential in Algeria, marked an important progress in palm trees date cultivars, which reached 18 million of palm trees, covering more than 350,000 ha, where 11 million trees are productive and producing approximately 492,000 tons of dates (Statistics of the FAO, on 2015). The rest (residues) of the dates, which constitutes the common dates, reaches 250,000 tons which are not appreciated by the society and is marketed with a lot of difficulty on the local markets. 30% of these residues are of not satisfactory quality and they are mostly used as ruminant feed for animal. The state of Adrar (Fig. 1) produced 91,360 tons of dates in 2016 coming from 2,775,000 of the palm trees date. Most of this production is exported to neighboring countries while the rest is either consumed locally or used

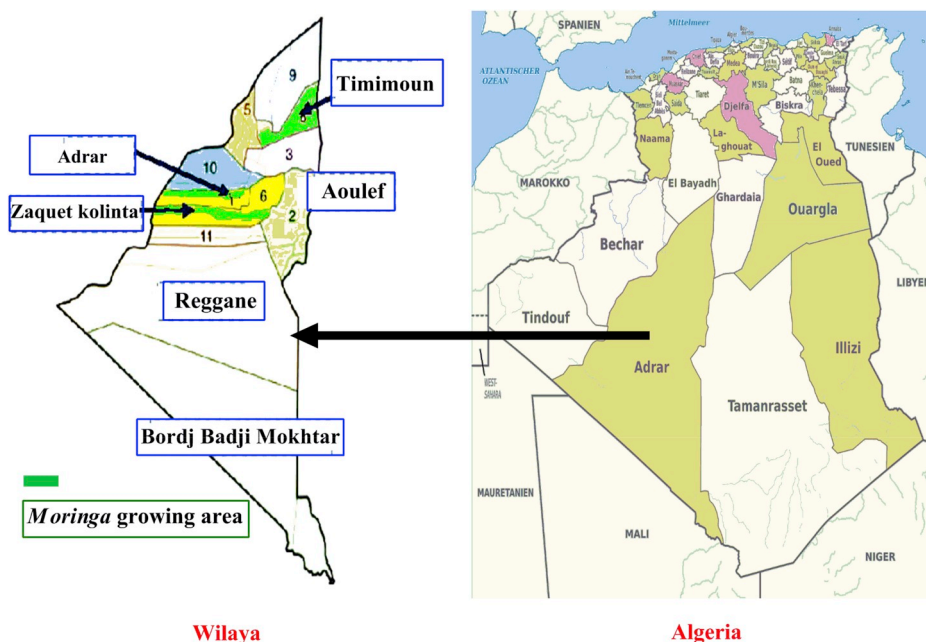


Fig. 1. Growing region of MO in Adrar state (Algeria).



Fig. 2. Photograph of *Moringa oleifera* tree and its seeds planted in Adrar state.

as animal feed. Fig. 3 shows common waste *Phoenix dactylifera* L. dates (WD) in Adrar state.

Based on the presented background, it is obvious that the cultivation of MO tree in addition to valorizing the WD can yield substantial benefits to the state of Adrar and Algeria in various aspects such as protecting the environment, preventing the degradation of the Saharan ecosystem and burial of oases by sand in addition to valorizing WD into useful biofuels. Therefore, this study aims to valorize both WD and MO trees to produce biodiesel from MO seeds (known as *Moringa oleifera* methyl ester, MOME) and BE from WD. This is followed by blending MOME and BE with Euro diesel (D) at various proportions with the aim of forming ternary fuel blends and improving their physicochemical properties such as density and cold flow properties. Furthermore, various analytical techniques such as gas chromatography (GC), Fourier transform infrared spectroscopy (FT-IR), thermogravimetric analysis (TGA) and differential scanning calorimetry (DSC) techniques to assess the quality of biodiesel, BE and the blends were examined and presented. It is believed that FT-IR, TGA and DSC techniques are used for the first time to assess the qualities of such blends. These techniques can be also adapted in the future as they are cheap, reliable and fast methods that can replace some expensive equipment used to assess the quality of biodiesel especially for oxidation degradation, cold flow properties and fuels identification, given that they are general equipment that can be easily found and accessible in many laboratories. Therefore, the successful outcome of this work may result in substantial benefits to the country as it is believed such a study is the first that aims to shadow the light into waste recycling in Algerian Saharan and state of Adrar. This will be helpful to the state to achieve a partial self-sufficiency in energy.

## 2. Material and methods

Analytical grade methanol (99%) and n-hexane were obtained from the Prochima Sigma, Algeria. MO seeds were collected from the Renewable Energy Research Unit, Adrar, Algeria. Prior to the oil extraction, the collected *Moringa* seeds were cleaned and dried in an oven at 80 °C for moisture removal.

### 2.1. Soxhlet extraction method

Soxhlet extraction apparatus was used to extract the oil from *Moringa oleifera* seeds. In this experiment, 300 mL of n-hexane was poured into a round bottom flask. About 10 g of powdered *Moringa oleifera* was placed in a thimble and inserted in the center of the extractor. The flask was heated until the boiling point of n-hexane. The vapor rises through the vertical tube into the condenser at the top. The liquid condensate drips into a filter paper thimble in the center, which contains the oil to be extracted. The extract seeps through the pores of the thimble and fills the siphon tube, where it flows back down into the round bottom flask. This was allowed to continue for the 30 min.

At the end of the extraction, the resulting mixture containing the oil and n-hexane was distilled off by simple distillation for oil recovery from solvent. The amount of oil extracted was then weighed to determine the oil content and finally stored in a glass bottle prior to biodiesel production.

### 2.2. Biodiesel production

Due to the high acid value (AV) of CMOO (AV = 9 mg KOH/g oil), biodiesel production process was conducted in two steps using H<sub>2</sub>SO<sub>4</sub> as strong acid catalyst to reduce the free fatty acid (FFA) to less than 1% in



Fig. 3. WD in Adrar state.

the esterification step, while KOH was used as a strong base catalyst to produce the methyl ester from the esterified oil, through transesterification reaction (Figs. 4 and 5). The reaction was carried out in a glass batch reactor equipped with a condenser to prevent methanol loss and the mixture was refluxed with simultaneous stirring at 600 rpm for 1 h.

After sampling, the mixture was allowed for phase separation (for at least 24 h). After phase separation, the traces of catalyst and alcohol were washed out with water from the mixture of esters until the water layer remains completely translucent. Finally, the ester layer was dried and analyzed.

### 2.3. Gas chromatography (GC) method of MOME (B100)

Fatty acid compositions of MOME was determined using gas chromatography (GC) (PerkinElmer Clarus 680) equipped with a flame ionization detector and a BPX70 capillary column. The test was conducted using an optimized in-house GC method (Atabani et al., 2015). The carrier gas was hydrogen with a column flow rate of 1.00 mL per minute. 1  $\mu$ L of the sample was injected into gas chromatography. Table 1 shows the summary of GC operating conditions.

### 2.4. Process for obtaining BE

- 1 Substrates: The choice of fermentation substrates depends on their availability in the South-West region, their abundance and their appreciation (high sugar content).
- 2 Biological material: The microorganism used is baker's yeast *Saccharomyces cerevisiae*. It is stored at 4 °C in a refrigerator (Buckner et al., 2011).
- 3 Preparation and washing of WD: The first step is the washing of the substrate with water to eliminate the dust and all other foreign

particles, the imbibition of the dates is done with the help of a hot water (90–95 °C) to facilitate coring, after removal of the cores, the pulps obtained are crushed. The paste obtained is then diluted with a ratio of 1 kg of dates per 4 L of water. The pH of the must is adjusted between 4.3 and 4.7 using sulfuric acid ( $H_2SO_4$ , 1 N) (The American Oil Chemists' Society (AOCS) 2005).

- 4 Alcoholic fermentation: After the medium has been inoculated with the baker's yeast *Saccharomyces cerevisiae*, the bioreactor is filled with the must at 2/3 of its capacity (asphyxiation conditions) and it is placed in a water bath set at 37 °C. After 72 h, the fermentation is

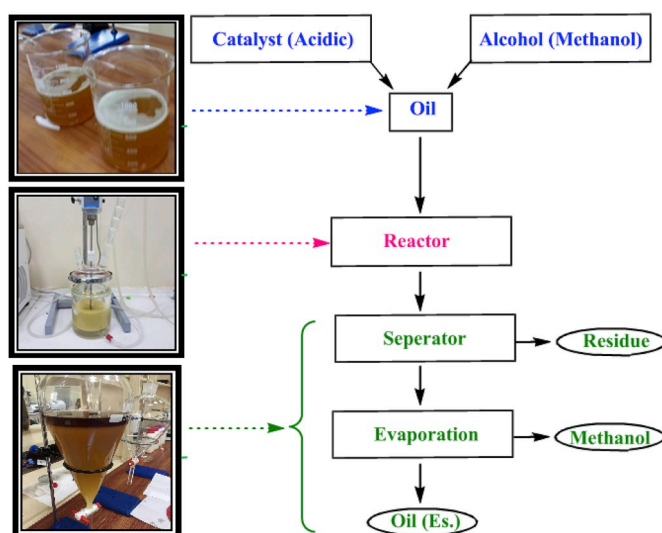


Fig. 4. Esterification steps for CMOO.

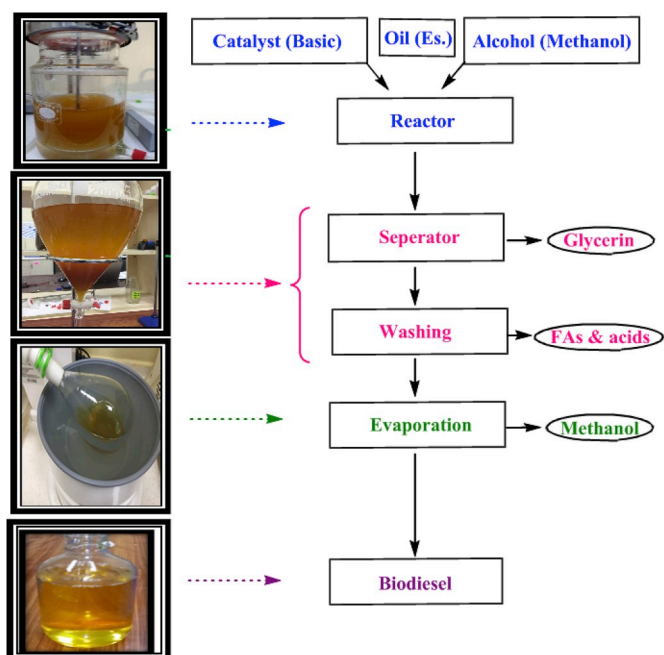


Fig. 5. Transesterification steps for the esterified oil.

**Table 1**  
GC operating conditions (biodiesel).

Property	Specifications	Unit
Carrier gas	Hydrogen	
Flow rate	1.00 (column flow)	mL/min
Detector temperature	250	°C
Column head pressure	70 (flow control made)	kPa
Column dimension	BPX70	60.0 m × 0.25µm × 0.25 mm ID
Injector column oven	250	°C
Temperature ramp	60 (hold for 2 min) 10 °C/min 200 °C 5 °C/min 240 °C (hold for 7 min)	°C

stopped. Fig. 6 shows the experimental device used for alcoholic fermentation to obtain BE.

5 Distillation: At the end of the fermentation, WD is filtered and distilled in order to extract the bioethanol. The main distiller compositions are shown in Fig. 7.

- Distillation tank: It is a stainless-steel pot with a capacity of 30 L, which carries a manometer and a valve at the lid;
- Distillation column: It is a copper tube of 35 mm diameter and 1.5 m long, placed vertically on the lid of the pot.

## 2.5. GC method of BE

BE has been identified using gas chromatography (GC) (PerkinElmer Clarus 500), equipped with a flame ionization detector and a RTX capillary column. Table 2 shows the summary of GC operating conditions. Absolute ethanol was used as a standard.

## 2.6. Characterization of MOME (B100), BE and their blends

Table 3 shows the blend plan adopted for this study.

### 2.6.1. DSC analysis

DSC is used to determine the crystallization onset temperature of

the samples and can be plotted on the graph against heat flow. The DSC curves were obtained in a calorimeter model DSC Q20 with RCS90 coupled with a cooling system, both from TA Instruments. For each test,  $3 \pm 0.5$  mg of each sample was loaded in an aluminum pan and heat flow was measured differentially by comparing heat flow of an empty reference pan as a reference. The rate of heating/cooling was  $10 \text{ }^\circ\text{C min}^{-1}$  between  $-80 \text{ }^\circ\text{C}$  and  $20 \text{ }^\circ\text{C}$  under an inert nitrogen atmosphere ( $\text{N}_2$ ) with a flow rate of  $50 \text{ mL min}^{-1}$ . The MOME with CMOO, BE, D and their blends were analyzed by TA Q-2000 DSC under the flow of nitrogen. Each DSC test takes roughly 17 mins to complete a single cycle. All the results were then processed with the help of a TA Orchestrator, Version V7.2.2.1.

### 2.6.2. FT-IR analysis

The MOME (B100) along with their respective blends were characterized by the FT-IR (Bruker Tensor 27) in the range  $4500\text{--}400 \text{ cm}^{-1}$  and processed with a computer software program OPUS 7.2.139.1294. The resolution was  $4 \text{ cm}^{-1}$  and 32 scans.

### 2.6.3. TGA analysis

The thermogravimetric (TG) thermograms of MOME (B100) and their respective blends were recorded in a Shimadzu DTG 60H thermogravimetric analyzer using the platinum pans. A 10 mg of each sample was loaded into pans. After completing each analysis, platinum pan was cleaned well in order to make the pan ready for the next run. The temperature ranges from 25 to  $700 \text{ }^\circ\text{C}$  with a heating rate of  $10 \text{ }^\circ\text{C/min}$  under dry air atmosphere of  $100 \text{ mL/min}$  to determine the oxidative stability. Each sample takes almost an hour to complete. A maximum temperature of  $700 \text{ }^\circ\text{C}$  was used as the mass remains constant until the end of analysis and all the chemical reactions have been completed at this temperature. TGA curves were plotted to analyze the onset temperature of MOME (B100), BE100, D100 and their blends.

## 2.7. Characterization of WD after BE production

Table 4 depicted the methods associated to characterization of samples. The drying matter (DM) was determined by method Association of Official Agricultural Chemists (AOAC) 934.01 at  $100 \text{ }^\circ\text{C}$  for 24 h (Buckner et al., 2011). The crude fiber (CF) was measured in a filter crucible by following AOCS Ba 6a-05 method ((The American Oil Chemists' Society AOCS 2005)). Total ash content (TAC) was determined by using AOAC 942.05 method. The sample was heated at  $600 \pm 2 \text{ }^\circ\text{C}$  or 5 or 24 h (overnight) at  $550 \text{ }^\circ\text{C}$  in muffle furnace (Yemmireddy et al., 2013). Solid crude protein (SCP) was determined by AOAC 990.03 method. The borate-phosphate buffer was pre-heated to  $39 \text{ }^\circ\text{C}$  and added to the samples for SCP measurement (Thiex, 2009). Acid Detergent Lignin (ADL) content was determined by AOAC 973.18 and determination of fat (DF) was determined using AOAC 945.16.

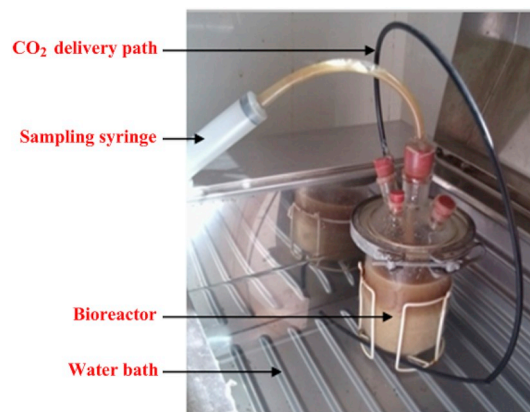


Fig. 6. Experimental device of alcoholic fermentation.

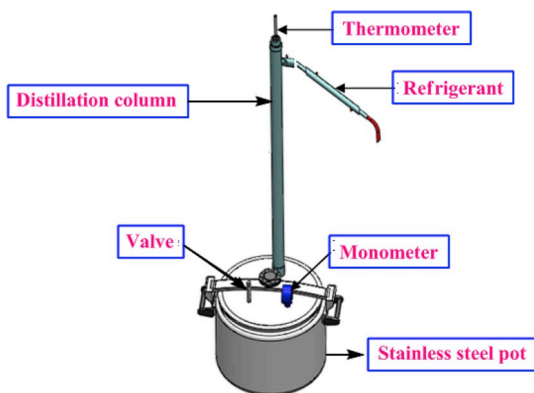


Fig. 7. Distillation device.

**Table 2**  
GC operating conditions (BE).

Property	Specifications	Unit
Carrier gas	Hydrogen	
Flow rate	4.00 (column flow)	mL/min
Detector temperature	150	°C
Column dimension	RTX	30.0 m × 0.25mm × 0.25 mm ID
Injector column oven	150	°C
Oven temperature	60	°C

**Table 3**  
Preparation of fuel blends (by volume).

Blend	Description
D100	100% D
MOME (B100)	100% MOME
D80B20	80% D + 20% MOME
D80BE20	80% D + 20% BE
B80BE20	80% MOME + 20% BE
D80B5BE15	80% D + 5% MOME + 15% BE
D80B10BE10	80% D + 10% MOME + 10% BE
D80B15BE5	80% D + 15% MOME + 5% BE

**Table 4**  
Description of methods used to measure DM, CF, TAC, SCP, Determination of Elements (DE), ADL and DF.

Property	Calculating Equation	Unit	Method	Ref
DM	$\%DM = \frac{\text{Dry Weight (g)}}{\text{Sample Fresh Weight (g)}} \times 100$	%	AOAC 934.01	1
CF	$\%CF = \frac{\text{Dry Weight (W}_1\text{)} - \text{Ash weight (W}_2\text{)}}{\text{Sample Weight (W}_0\text{)}} \times 100$	%	AOCS Ba 6a-05	2
TAC	$\%TAC = \frac{\text{Ash weight (g)}}{\text{Fresh Weight (g)}} \times 100$	%	AOAC 942.05	3
SCP	$SCP = \frac{(V_1 - V_0) \times 14.007 \times 6.25}{\text{Sample Weight (g)}} \times 100$	gPr/L	AOAC 990.03	4
DE	$ppm (mg/L) = \frac{ppm (from calibration graph) \times D}{\text{Sample Weight (g)}} \times 100$ In % = ppm in sample × 0.0001 $D = \frac{\text{Total volume}}{\text{Volume taken}}$	ppm/mg/L	–	5
ADL	$\%ADL = \frac{(W_2 - W_3)}{W_1} \times 100$ W1 = weight of sample (g) W2 = weight of crucible and residue after drying (g) W3 = weight of crucible and residue after ashing (g)	%	AOAC 973.18	6
DF	$\%Fat = \frac{(\text{Flask wt after extraction}) - (\text{Flask wt before extraction})}{\text{Sample Weight (g)}} \times 100$	%	AOAC 945.16	4

<sup>1</sup>Buckner et al., 2011.<sup>2</sup>AOCS, 2005.<sup>3</sup>Yemmireddy et al., 2013.<sup>4</sup>Thiex, 2009.<sup>5</sup>Yang et al., 2013.<sup>6</sup>Möller, 2009.

**Table 5**  
CMOO characteristics.

Property	Results	CMOO <sup>a</sup>	SCGO <sup>b</sup>	WCO/SCGO <sup>b</sup>
Cloud point (°C)	15	10	−3	5
Pour point (°C)	13	11	−3	2
Density at 15 °C (kg/m <sup>3</sup> )	914.8	–	932.9	923.7
Density at 20 °C (kg/m <sup>3</sup> )	911	–	–	–
Density at 25 °C (kg/m <sup>3</sup> )	907.5	–	–	–
Density at 30 °C (kg/m <sup>3</sup> )	904	–	–	–
Density at 40 °C (kg/m <sup>3</sup> )	896.7	897.5	–	–
Acid value (mg NaOH/g oil)	9.04	8.62 <sup>†</sup>	22.3	12.1

\*Measured in mg KOH/g oil.

<sup>a</sup> Mofijur et al., 2014b.<sup>b</sup> Atabani et al., 2019b.

### 3. Results and discussion

#### 3.1. Physico-chemical properties of CMOO

The oil content of *Moringa oleifera* seeds was 40% by weight of dry seeds, this result is very similar to several studies in the literature such as; 40.0% (Oliveira et al., 2012), 41% (Domínguez et al., 2017), 35% w/w (Anwar et al., 2005; Rashid et al., 2008). 36.48% (Pereira et al., 2016a), and 34.5% (Goja, 2013). Table 5 shows some results of CMOO properties, besides a comparison with the results of (Mofijur et al., 2014b).

A density of CMOO is 896.7 kg/m<sup>3</sup> which is less than the value of (Mofijur et al., 2014b) 897.5 kg/m<sup>3</sup>. Acid number measures the presence of FFA's, generated by effects of the hydrolysis or oxidative reaction pathway. The conditions of production and storage of the seeds, the expiry date, the processing time and the means of manipulation favor the increase of this number (Pereira et al., 2016b).

The results obtained show a high acid number (9.04 mg NaOH/g oil) which require two successive operations to convert the CMOO into biodiesel (Esterification and trans-esterification). However, this result is very similar to (Mofijur et al., 2014b) (8.62 mg KOH/g oil) and extremely lower compared to other feedstocks from waste such as spent coffee grounds oil (SCGO) and mix of waste cooking oil and spent coffee grounds oil (WCO/SCGO) (50/50% volume).

### 3.2. Fatty acid compositions (FAC) and biodiesel characteristics

The obtained MOME (B100) yield is 91%. The results of FAC are summarized and compared with (Mofijur et al., 2014a) in Table 6. It can be seen that the monounsaturated fatty acid content (74.16%) is much higher than its content of saturated fatty acids (25.20%) and polyunsaturated fatty acids (0.63%). Oleic acid is the highest content (74.16%), followed by palmitic acid (7.01%). These results are well agreed with (Mofijur et al., 2014a). In comparison to other feedstocks, it has been observed that MOME has similar saturation level compared to *Calophyllum inopohyllum* methyl ester (CIME) (25%) (Ashok et al., 2017; Nanthagopal et al., 2018), while monounsaturated fatty acid content was 50% and polyunsaturated fatty acids was (25%) compared to 74.16% and only 0.63% of MOME respectively.

The properties of the MOME, besides a comparison with (Mofijur et al., 2014a) and our previous study (Atabani et al., 2019b) for waste cooking/spent coffee grounds oils methyl ester (WCOME/SCGOME) are given in Table 7.

### 3.3. GC results of BE

The results obtained by GC analysis indicated a high percentage of BE (96.83%) and 3.17% of impurities, see (Fig. 8) and annex.

### 3.4. IR results of BE

IR spectra of BE is shown in Fig. 9 and the summary is tabulated in Table 8. Some important bands in the IR spectrum can be seen at  $3400\text{ cm}^{-1}$  corresponding to  $\nu(\text{-OH})$ . It manifests itself by a strong and wide absorption band. It can be explained by the presence of a hydroxyl group associated by hydrogen bond (ethanol in solution).

An absorption band at  $2900\text{ cm}^{-1}$  is attributed to the  $\nu(\text{-CH})$  binding elongation. This band is in concordant with the  $\text{-CH}_2$  and  $\text{-CH}_3$  linkage elongation vibrations. The elongation at the C–O bond of the primary alcohol (Ethanol) is also characterized by the presence of an absorption band at  $\nu(\text{-C-O})$   $1100\text{ cm}^{-1}$ . The infrared spectrum (Fig. 9) and the chromatogram (Fig. 8) confirm the structure and the functional groups exist in the BE molecule, perfectly.

### 3.5. Characterization of biodiesel and its blends

Table 9 shows some examined properties of MOME and its blends with D and BE. The positive effect of blending alcohol in reducing the density of MOME is obvious. This is in agreement with (Ashok et al., 2019) where the increasing percentage of octanol in CIME remarkably reduced the density. All that proves the positive aspect of introducing alcohols to CI engines along with biodiesel. It can be seen that the

**Table 6**  
FAC of MOME (B100).

Fatty acid	Molecular weight	Structure	Systematic name	Formula	MOME (%)	1 (%)
Myristic	228	14:00	Tetradecanoic	$\text{C}_{14}\text{H}_{28}\text{O}_2$	0.63	0.1
Palmitic	256	16:00	Hexadecanoic	$\text{C}_{16}\text{H}_{32}\text{O}_2$	7.01	7.9
Palmitoleic	254	16:01	Hexadec-9-enoic	$\text{C}_{16}\text{H}_{30}\text{O}_2$	0	1.7
Stearic	284	18:00	Octadecanoic	$\text{C}_{18}\text{H}_{36}\text{O}_2$	6.48	5.5
Oleic	282	18:01	Cis-9-Octadecenoic	$\text{C}_{18}\text{H}_{34}\text{O}_2$	74.16	74.1
Linoleic	280	18:02	Cis-9-cis-12 Octadecadienoic	$\text{C}_{18}\text{H}_{32}\text{O}_2$	0.63	4.1
Linolenic	278	18:03	Cis-9-cis-12	$\text{C}_{18}\text{H}_{30}\text{O}_2$	0	0.2
Arachidic	312	20:00	Eicosanoic	$\text{C}_{20}\text{H}_{40}\text{O}_2$	4.38	2.3
Eicosanoic	310	20:01	Cis-11-eicosenoic	$\text{C}_{20}\text{H}_{38}\text{O}_2$	0	1.3
Behenic	340	22:00	Docosanoic	$\text{C}_{22}\text{H}_{44}\text{O}_2$	6.70	2.8
<b>Saturated acids (%)</b>					<b>25.2</b>	<b>18.6</b>
<b>Monounsaturated acids (%)</b>					<b>74.16</b>	<b>77.1</b>
<b>Polyunsaturated acids (%)</b>					<b>0.63</b>	<b>4.3</b>
<b>Total (%)</b>					<b>100</b>	<b>100</b>

<sup>1</sup> Mofijur et al., 2014a.

**Table 7**  
Properties of MOME (B100).

Property	MOME	MOME <sup>a</sup>	WCOME/SCGOME <sup>b</sup>
Cloud point (°C)	20	19	9
Pour point (°C)	22	19	9
Density at 15 °C (kg/m <sup>3</sup> )	881.9	–	885
Density at 20 °C (kg/m <sup>3</sup> )	873.7	–	881.3
Density at 25 °C (kg/m <sup>3</sup> )	870	–	877.6
Density at 30 °C (kg/m <sup>3</sup> )	866.3	–	873.8
Density at 40 °C (kg/m <sup>3</sup> )	859.1	869.6	866.5
Cold filter plugging point (°C)	10	18	2
Saponification number <sup>c</sup>	197.08	199	204.8
Iodine value <sup>a</sup> (g I/100 g)	69.27	77.5	83.71
Cetane number <sup>a</sup>	58.36	56.3	56.64
Higher heating value <sup>a</sup> (MJ/kg)	39.52	40.05	39.44
Oxidation stability <sup>a</sup> (h)	7.21	26.2	6.51

<sup>a</sup> (Mofijur et al., 2014a).

<sup>b</sup> (Atabani et al., 2019b).

<sup>c</sup> Results were calculated empirically (Mohammed et al., 2018).

blends D80BE20 and D80B5BE15 possess the values of cloud point, pour point and density close to that of the D.

Fig. 10 and Table 10 show the variation of densities of CMOO, MOME, BE and D against temperatures (15–40 °C) along with developed formulae to predict the density at any temperature, in this range. It can be seen that density of fuels decreases with increasing temperature. The results also show that BE has densities very close to D, whereas the MOME has the density values less than its crude oil (CMO) and higher than D and BE. These results justify the choice of the proportion of ternary blends for the three fuels viz. D, BE and MOME.

#### 3.5.1. DSC analysis

The crystallization onset temperatures of MOME (B100), BE100, D100 and their blends under N<sub>2</sub> atmosphere were studied using DSC and are presented in Table 11.

The crystallization onset temperatures for MOME (B100), D100 and BE100 are 17.07 °C, –5.10 °C and –57.17 °C respectively. Hence, biodiesel crystallizes faster than D and BE. The crystallization onset temperatures of D80B5BE15, D80B10BE10, D80B15BE5, D80B20 and CMOO are –6.49 °C, –4.45 °C, –2.32 °C, –0.29 °C and 8.58 °C respectively. It can be seen that as the biodiesel ratio increases, the crystallization temperature also increases (Kandala, 2009). The crystallization onset temperature of B80BE20 and D80BE20 are 16.92 °C, and –10,13 °C respectively.

#### 3.5.2. FT-IR analysis

Fig. 11 displays the infrared spectra of MOME (B100) and CMOO, BE100, D100 and their blends. In FT-IR, the ester carbonyl group

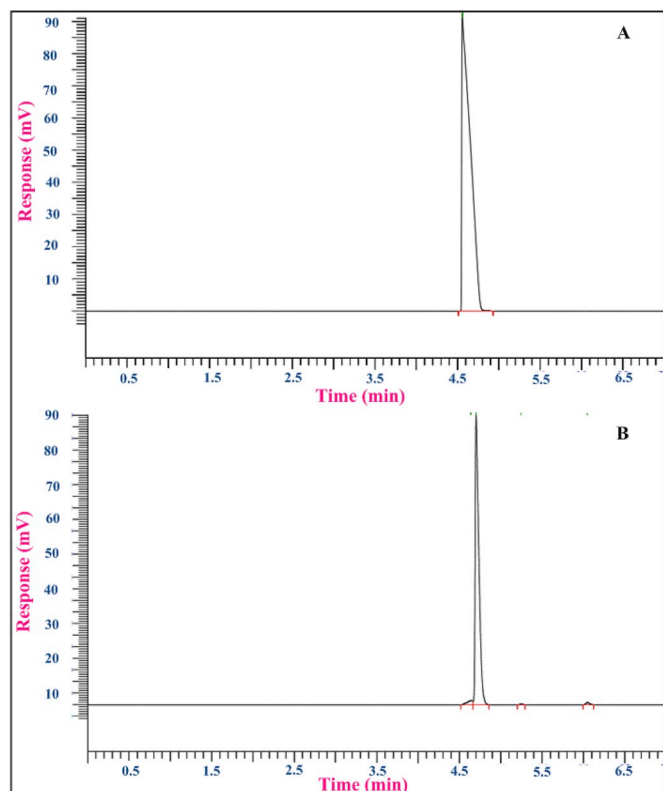


Fig. 8. Chromatograph (A: Pure Ethanol, B: BE).

stretching  $\nu(\text{C}=\text{O})$  shows strong bands at nearly  $\sim 1739\text{ cm}^{-1}$  to monitor the progress of the reaction (O'Donnell et al., 2013; Rabelo et al., 2015). The esteric (CO-C) vibration between at  $1161.08$  and  $1045.11\text{ cm}^{-1}$  reveals medium intensity bands, and the presence of the  $\nu(-\text{CH}_2)_n$  group vibration band is seen at nearly  $721.90\text{ cm}^{-1}$ . The peak at nearly  $1385\text{ cm}^{-1}$  corresponds to the asymmetric stretching of  $\nu^{\text{asym}}(-\text{CH}_3)$ . The stretching of  $\nu(\text{O}-\text{CH}_3)$ , represented by the absorbance at  $1161.08\text{ cm}^{-1}$ , is typical of biodiesel. The  $3332\text{ cm}^{-1}$  broad strong band indicates O-H stretching in BE.

### 3.5.3. TGA analysis

Oxidative stability of MOME (B100) and its blends with D100 and BE100 were quantified by Thermogravimetric analysis (TGA). It (TGA) is a technique for characterizing the thermal and oxidative stability of a material (compound or mixture) by measuring changes in its physico-chemical properties. These properties were expressed in terms of weight change as a function of increasing temperature. The oxidative stability is a quality indicator parameter for esters. Thermogravimetric curves (TGA) show the weight loss at different temperatures and the first derivative of the weight loss in relation to the temperature curves.

Table 8

The following table groups together the important bands in the spectrum IR.

Frequency	Group	Intensity
3400	O-H elongation band $\nu(\text{O}-\text{H})$	Strong, wide
2900	C-H elongation band $\nu(-\text{CH}_3, -\text{CH}_2)$	Medium
1100	C-O elongation band $\nu(\text{C}-\text{O})$	Medium

Fig. 12(a) and, Fig. 12(b) show the TGA/DTGA curves for MOME (B100) and its blends with D100 and BE100. MOME (B100) trend did not depicted any declination before  $150\text{ }^\circ\text{C}$ , which revealed and confirmed its affirmative stability. It can be seen that the oxidative degradation occurred in a single continuous step in the temperature range of  $130.3\text{--}214.3\text{ }^\circ\text{C}$  for MOME (B100) and its blends with both D100 and BE100. The rapid declined in the graph steep by altering the slope of the curve was observed. This could be attributed by rate of mass change with respect to temperature, which due to evaporation and cracking phenomena. The graph slope did not show any significance about the progress of distillation weight loss or it is due to the previous thermal cracking of samples. The onset temperature ( $T_{\text{onset}}$ ) defined the sample weight loss thermally at transition phase. Therefore,  $T_{\text{onset}}$  can give the idea of initial boiling point of the samples besides the thermal stability. The low polyunsaturation and incremented oxidation stability of samples exhibits higher  $T_{\text{onset}}$  value. In these temperature ranges, the mass losses occur at levels of  $91.0\text{--}98.2\%$ . While oxidative degradation occurred at  $234.5\text{ }^\circ\text{C}$  for MOME (B100),  $54.2\text{ }^\circ\text{C}$  for BE100,  $137.3\text{ }^\circ\text{C}$  for D100 and  $345.9\text{ }^\circ\text{C}$  for CMOO. In these temperature ranges, the mass losses occur at levels of  $96.3\%$ ,  $97.6\%$ ,  $98.7\%$  and  $98.7\%$  for MOME (B100), BE100, D100 and CMOO respectively. The results of the oxidation onset temperatures were represented in Table 12. It can be observed that the oxidative stability increases as the biodiesel ratio increases in the blend.

### 3.6. Chemical composition of WD after ethanol production

Table 13 demonstrates the chemical compositions of WD and compared with spent coffee ground (SCG) and defatted spent coffee grounds (DSCG) as wastes. The dry matter (DM) issue content varies from  $85.85$  to  $92.51\%$ . SCG had the most elevated DM and WD the least, with no noteworthy contrast with DSCG. The outcomes are equivalent to those revealed already with certain identification with date assortment and agro-climatic and ecological conditions (Assirey, 2015). The crude protein content went from  $0.1855\text{ gm/L}$  in the WD to  $0.359\text{ gm/L}$  in SCG, showing moderately little protein in WD; it has been accounted for beforehand that dates are not a decent wellspring of protein. No noteworthy contrast in protein content was seen between two gatherings of cultivars: Shalaby, Khodari, Labanah and Anabarah and Ajwa, Sukkari, Suqaey, Safawy and Burni. The Mabroom

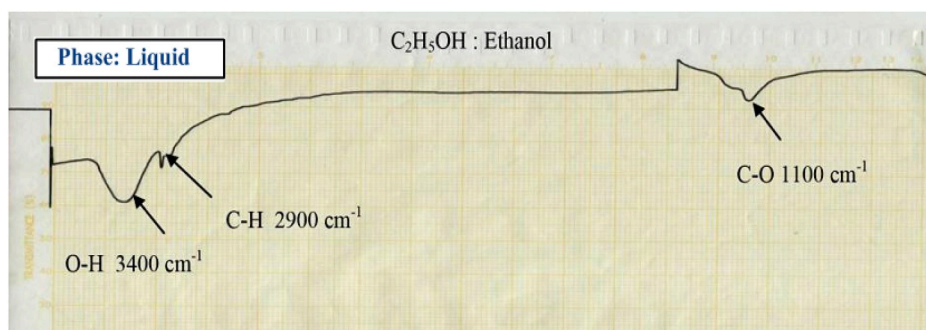
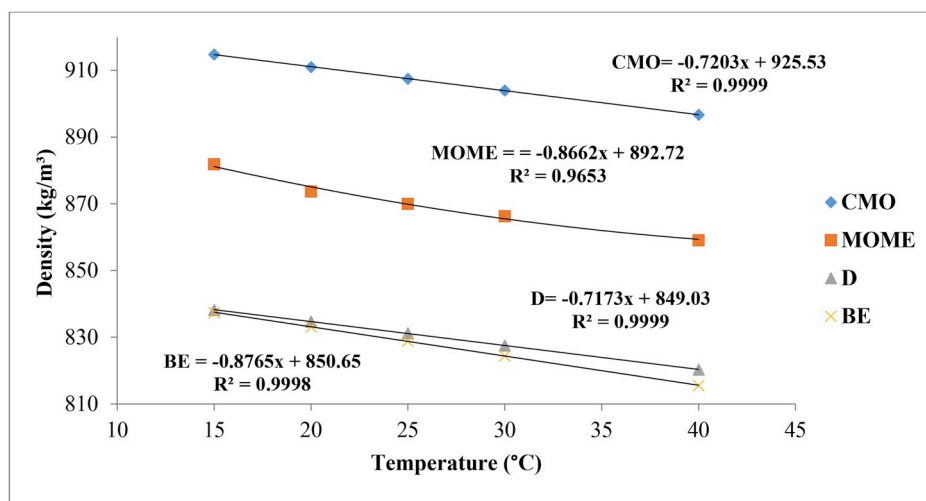


Fig. 9. Infrared spectra of BE.

**Table 9**  
Characteristics of MOME-BE-D blends.

Property	D80B20	D80BE20	B80BE20	D80B10BE10	D80B15BE5	D80B5BE15	D	MOME	CMOO
Cloud point (°C)	6	-7	21	-1	-0.1	-5	-5	20	15
Pour point (°C)	-16	-25	19	-18	-17	-24	-24	22	13
Density at 15 °C (kg/m <sup>3</sup> )	849.4	836.9	872.5	840.7	843	838.6	838.2	881.9	914.8
Cold filter plugging point (°C)	-23	-32	0	-28	-25	-29	-33	10	-



**Fig. 10.** Variations of density as a function of temperature for different fuels (15–40 °C).

**Table 10**  
Evaluation of density (kg/m<sup>3</sup>) as a function of temperature for different fuels.

Type	15 °C	20 °C	25 °C	30 °C	40 °C
CMOO	914.8	911	907.5	904	896.7
MOME	881.9	873.7	870	866.3	859.1
D	838.2	834.7	831.2	827.5	820.3
BE	837.4	833.1	828.9	824.4	815.5

**Table 11**  
Crystallizations onset temperature (°C) of MOME (B100), CMOO, BE, D and their blends under N<sub>2</sub> atmosphere.

Samples	Crystallizations onset temperature (°C)
MOME (BE100)	-57.17
MOME	17.07
D100	-5.10
D80B5BE15	-6.49
D80B10BE10	-4.45
D80B15BE5	-2.32
B80BE20	16.92
D80BE20	-10.13
D80B20	-0.29
CMOO	8.58

assortment had the most minimal protein content (Al-Hooti et al., 1997). These findings support that WD are useless as ruminant feed. Therefore, production of BE is more effective way to valorize WD in Algerian saharan as proposed in this study.

The WD tests demonstrated invalid fat substance, while SCG fat substance is 15 folds higher. It was accounted for an extremely low fat substance, from 0.12 g/100 g dry issue in Safawy to 0.72 g/100 g in Labanah. The information announced beforehand for dates created in Saudi Arabia (Sawaya et al., 1983) and in the United Arab Emirates (Ahmed et al., 1995) and in some Iranian assortments (0.4–0.9% of fat). There is no critical contrast in fat substance was accounted for in Anabarah, Sukkari, Suqaey, Burni and Labanah dates.

The ash content extended from 6.0323 %gm is acquired for WD, which is quite higher than reported in literature i.e. 1.68 gm in Safawy to 3.94 g in Labanah dates. 1.68 gm in Safawy to 3.94 g in Labanah dates (Assirey, 2015).

WD and SCG contained critical measures of minerals. The calcium focus was the most noteworthy (27.20 gm/L) followed in dropping by magnesium (16.31 gm/L). Comparable outcomes were accounted by (Assirey, 2015), and current outcomes are in close concurrence with those of numerous different investigations, which demonstrate that dates contain reasonable centralizations of calcium, potassium and phosphorus, which are significant for digestion in human cells (Al-Hooti et al., 1997). Magnesium and calcium are fundamental for solid bone improvement and for vitality digestion, and iron is basic for red platelet creation. The high potassium and low sodium substance of dates are reasonable for individuals with hypertension. A large portion of the examined minerals demonstrated noteworthy contrast among the various assortments, particularly for potassium. The varieties in magnesium and sodium substance could be clarified by components, for example, assortment, soil type and measure of manure. The WD didn't demonstrate any huge outcomes for lignin (Assirey, 2015).

#### 4. Conclusion

This article adopted a modern technique to simultaneously protect the environment and produce alternative fuels from the Saharan environment in Algeria. *Moringa oleifera* seeds have been valorized to produce biodiesel, while waste date seeds were also valorized into bioethanol rather than being used as animal feed. Both produced bio-fuels were characterized for some physicochemical properties, followed by blending at different percentages with Euro diesel. Moreover, GC, FT-IR, TGA and DSC techniques were adopted in this study as modern techniques to assess the quality of biofuels. The obtained results show 40% high oil content of *Moringa oleifera* seeds, 91% biodiesel yield and 96.83% bioethanol with 3.17% of impurities. Biodiesel from *Moringa oleifera* has been found to have high cloud, pour and cold filter plugging points of 20, 22 and 10 °C respectively. This is due to its high saturation

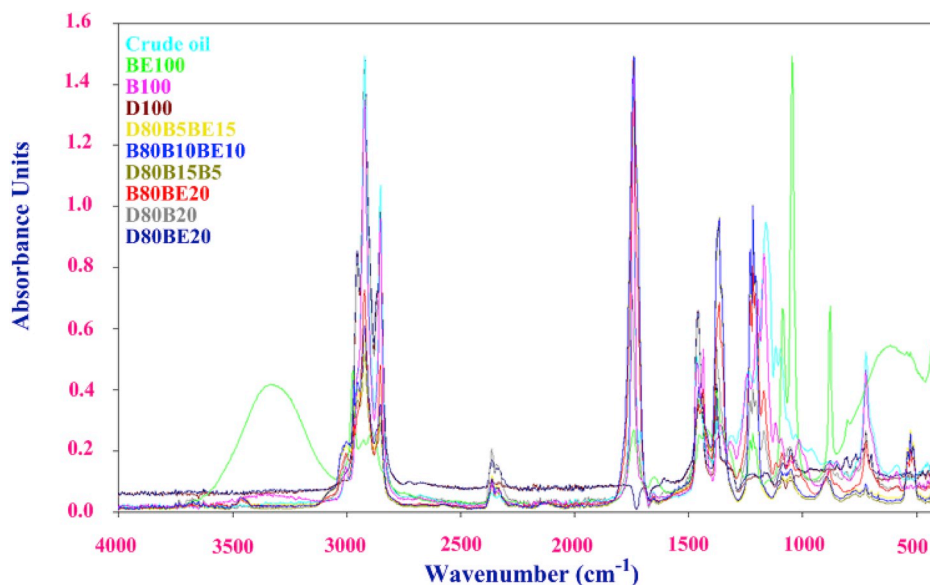
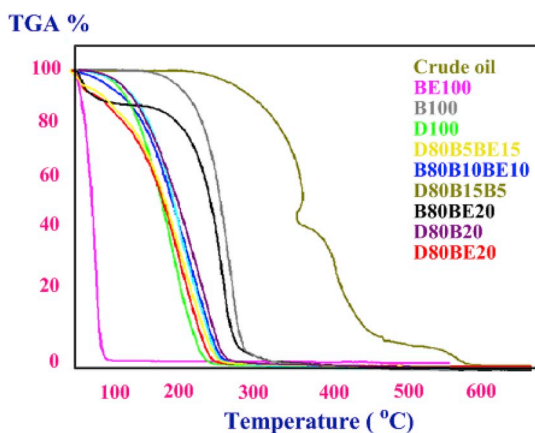
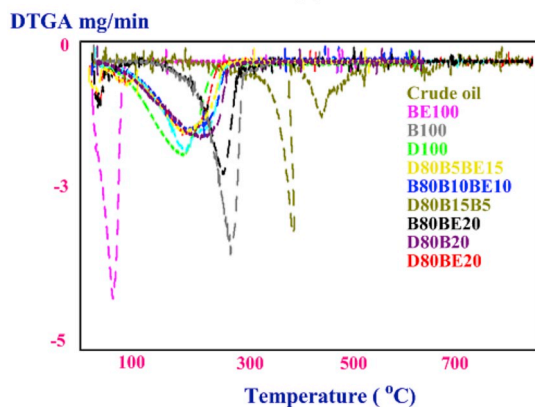


Fig. 11. Infrared spectra of MOME (B100), BE100, D100 and their blends.



(a)



(b)

Fig. 12. (a) Thermogravimetric analyses (TGA) of MOME (B100), D100, BE100 and their blends for oxidative stability. (b) Derivative Thermogravimetric analyses (DTGA) of MOME (B100), D100, BE100 and their blends for oxidative stability.

level (77.1%). This high saturation also caused biodiesel to have high oxidation stability, cetane number of 7.21 h and 58.36 and low iodine value of 69.27 (g I/100 g). Thus, blending with Euro diesel and

Table 12

TGA Analysis of MOME (B100) and its blends with D100 and BE100.

Sample name	Heating rate (°C/min)	Temperature Ranges (°C)	Onset temperature for thermal degradation (°C)	Mass loss under dry air (%)
MOME (B100)	10	180–330	234.5	96.3
B80BE20	10	120–330	214.3	95.2
D80B20	10	100–270	147.1	91.0
D80B15BE5	10	95–290	143.2	97.6
D80B10BE10	10	40–270	130.3	98.2
D80B5BE15	10	20–250	162.6	96.0
BE100	10	20–75	54.2	97.6
D80BE20	10	45–270	125.9	98.2
D100	10	85–250	137.3	98.7
CMOO	10	200–650	345.9	98.7

bioethanol has improved the pour point (19 to  $-24$  °C), cold filter plugging point (0 to  $-29$  °C) and density ( $838.6$ – $872.5$  kg/m<sup>3</sup>) compared to  $881.9$  kg/m<sup>3</sup> of Moringa biodiesel.

Some of the key findings of this study are summarized as below:

- 1 The GC tests confirm the existence of both biodiesel and bioethanol in all blends.
- 2 As the percentage of biodiesel ratio increases, the crystallization temperature increases due to the high cloud and pour points of *Moringa oleifera* biodiesel.
- 3 The oxidative stability increases as the biodiesel ratio in the blend increases.
- 4 The best proportions were found for the ternary blends of D80B5BE15, D80B10BE10 and D80B15BE5 which exhibit similar densities and cold flow properties values to those of Euro-diesel.
- 5 Our analysis proved that waste dates are useless as ruminant feed due to low protein content.

In conclusion, the study proved the valorization opportunities of both *Moringa oleifera* and waste date seeds to produce biodiesel and bioethanol in the Algerian Saharan. Thus, policy maker of the country shall implement some serious plan to realize the application of both sources to produce biofuels in Algeria.

**Table 13**  
Chemical composition of WD after ethanol production.

Waste	DM (%gm)	Fiber (%gm)	Soluble protein (gm/L)	Ash (%gm)	Magnesium (gm/L)	Calcium (gm/L)	Moisture (%gm)	Fat (%gm)	Lignin (%gm)
WD	85.85	9.8957	0.1855	6.0323	16.31	27.20	14.15	–	–
SCG	91.29	24.4583	0.359	1.5492	20.99	10.2	8.71	15.6041	12.0207
DSCG	92.51	23.4583	0.2845	1.8289	16.85	8.91	7.49	1.6896	11.1182

## References

- Ahmed, I.A., Ahmed, A.-W.K., Robinson, R.K., 1995. Chemical composition of date varieties as influenced by the stage of ripening. *Food Chem.* 54 (3), 305–309.
- Al-Hooti, S., Sidhu, J.S., Qabazard, H., 1997. Physicochemical characteristics of five date fruit cultivars grown in the United Arab Emirates. *Plant Foods Hum. Nutr.* 50 (2), 101–113.
- Anwar, F., Ashraf, M., Bhangar, M.I., 2005. Interprovenance variation in the composition of *Moringa oleifera* oilseeds from Pakistan. *J. Am. Oil Chem. Soc.* 82 (1), 45–51.
- Anwar, F., Zafar, S.N., Rashid, U., 2006. Characterization of *Moringa oleifera* seed oil from drought and irrigated regions of Punjab, Pakistan. *Grasas Aceites* 57 (2), 160–168.
- Ashok, B., Nanthagopal, K., Anand, V., Aravind, K.M., Jeevanantham, A.K., Balusamy, S., 2019. Effects of n-octanol as a fuel blend with biodiesel on diesel engine characteristics. *Fuel* 246, 363–363.
- Ashok, B., Nanthagopal, K., Jeevanantham, A.K., Bhowmick, P., Malhotra, D., Agarwal, P., 2017. An assessment of calophyllum inophyllum biodiesel fuelled diesel engine characteristics using novel antioxidant additives. *Energy Convers. Manag.* 148, 935–943.
- Assirey, E.A.-R., 2015. Nutritional composition of fruit of 10 date palm (*Phoenix dactylifera* L.) cultivars grown in Saudi Arabia. *J. Taibah Univ. Sci.* 9 (1), 75–79.
- Atabani, A.E., Silitonga, A.S., Badruddin, I.A., Mahlia, T.M.I., Masjuki, H.H., Mekhilef, S., 2012. A comprehensive review on biodiesel as an alternative energy resource and its characteristics. *Renew. Sustain. Energy Rev.* 16 (4), 2070–2093.
- Atabani, A.E., Mahlia, T.M.I., Masjuki, H.H., Badruddin, I.A., Anjum, Wan Yusof, Hafizzudin, Chong, W.T., Lee, K.T., 2013a. A comparative evaluation of physical and chemical properties of biodiesel synthesized from edible and non-edible oils and study on the effect of biodiesel blending. *Energy* 58 (September), 296–304.
- Atabani, A.E., Silitonga, A.S., Ong, H.C., Mahlia, T.M.I., Masjuki, H.H., Badruddin, I.A., Fayaz, H., 2013b. Non-edible vegetable oils: a critical evaluation of oil extraction, fatty acid compositions, biodiesel production, characteristics, engine performance and emissions production. *Renew. Sustain. Energy Rev.* 18 (February), 211–245.
- Atabani, A.E., Badruddin, Irfan Anjum, Masjuki, H.H., Chong, W.T., Lee, K.T., 2015. Pangium edule Reinw: a promising non-edible oil feedstock for biodiesel production. *Arabian J. Sci. Eng.* 40 (2), 583–594.
- Atabani, A.E., Al-Muhtaseb, A.H., Kumar, G., Saratale, G.D., Aslam, M., Khan, A.B., Said, Z., Mahmoud, E., 2019a. Valorization of spent coffee grounds into biofuels and value-added products: pathway towards integrated bio-refinery. *Fuel* 254, 115640.
- Atabani, A.E., Shobana, S., Mohammed, M.N., Uguz, G., Kumar, G., Aravindnarayan, S., Aslam, M., Al-Muhtaseb, A.H., 2019b. “Integrated valorization of waste cooking oil and spent coffee grounds for biodiesel production: blending with higher alcohols, FT-IR, TGA, DSC and NMR characterizations. *Fuel* 244, 419–430.
- Buckner, C.D., Wilken, M.F., Benton PAS, J.R., Vanness, S.J., Bremer, V.R., Klopfenstein, T.J., Kononoff, P.J., Erickson PAS, G.E., 2011. Nutrient variability for distillers grains plus solubles and dry matter determination of ethanol by-products. *Prof. Anim. Sci.* 27 (1), 57–64.
- Dominguez, Y.D., García, D.T., Pérez, L.G., 2017. Extraction and characterization of oil from *Moringa oleifera* for energy purposes. *Wulfenia J.* 24 (5), 86–103.
- Goja, A.M., 2013. Physico-chemical properties of oil produced from *Moringa oleifera*, *Jatropha curcas* and *Carthamus tinctorius* L seeds. *Int. J. Adv. Res.* 1 (4), 181–187.
- Hsu, R., Midcap, S., Arbainsyah, M., De Witte, L., 2006. *Moringa oleifera*; Medicinal and Socioeconomic Uses. International Course on Economic Botany. National Herbarium, Leiden, the Netherlands Retrieved 20th April, 2018, from: <https://miracletrees.org/moringa-medicinal-socio-economic-uses.html>.
- Kandala, H., 2009. The study of variations. In: *The Properties of Biodiesel on Addition of Antioxidants*. Department of Chemistry. Western Kentucky University Bowling Green, Kentucky, USA (Kentucky. Master of Science).
- Keskin, A., Yaşar, A., Reşitoğlu, I., Akar, M.A., Sığözü, I., 2013. The influence of diesel fuel-biodiesel-ethanol/butanol blends on the performance and emission characteristics of a diesel engine. *Energy Sources, Part A Recovery, Util. Environ. Eff.* 35, 1873–1881.
- Labeckas, G., Slavinskas, S., Mazeika, M., 2014. The effect of ethanol–diesel–biodiesel blends on combustion, performance and emissions of a direct injection diesel engine. *Energy Convers. Manag.* 79, 698–720.
- Lalas, S., Tsaknis, J., 2002. Characterization of *Moringa oleifera* seed oil variety “Periyakulam 1”. *J. Food Compos. Anal.* 15 (1), 65–77.
- Machell, K., 1994. Report on the extraction of *Moringa* oil from *Moringa* oil seeds. Intermediate Technology Zimbabwe. Harare, Zimbabwe.
- Mofijur, M., Masjuki, H.H., Kalam, M.A., Atabani, A.E., Arbab, M.I., Cheng, S.F., Gouk, S.W., 2014a. Properties and use of *Moringa oleifera* biodiesel and diesel fuel blends in a multi-cylinder diesel engine. *Energy Convers. Manag.* 82, 169–176.
- Mofijur, M., Masjuki, H.H., Kalam, M.A., Atabani, A.E., Rizwanul Fattah, I.M., Mobarak, H.M., 2014b. Comparative evaluation of performance and emission characteristics of *Moringa oleifera* and Palm oil based biodiesel in a diesel engine. *Ind. Crops Prod.* 53, 78–84.
- Mohammed, A.S., Lai, O.M., Muhammad, S.K.S., Long, K., Ghazali, H.M., 2003. *Moringa oleifera*, potentially a new source of oleic acid-type oil for Malaysia. *Invest. Innovat.* 3, 137–140.
- Mohammed, M.N., Atabani, A.E., Uguz, G., Lay, C.H., Kumar, G., Al-Samarae, R.R., 2018. Characterization of Hemp (*Cannabis sativa* L.) biodiesel blends with Euro diesel, butanol and diethyl ether using FT-IR, UV-Vis, TGA and DSC techniques. *Waste and Biomass Valorization* 1–17 (Article in press).
- Möller, J., 2009. Gravimetric determination of acid detergent fiber and lignin in feed: interlaboratory study. *J. AOAC Int.* 92 (1), 74–90.
- Nanthagopal, K., Ashok, B., Varatharajan, V., Anand, V., Dinesh Kumar, R.D., 2017. “Study on the effect of exhaust gas-based fuel preheating device on ethanol–diesel blends operation in a compression ignition engine. *Clean Technol. Environ. Policy* 19, 2379–2392.
- Nanthagopal, K., Ashok, B., Saravanan, B., Korah, S.M., Chandra, S., 2018. Effect of next generation higher alcohols and Calophyllum inophyllum methyl ester blends in diesel engine. *J. Clean. Prod.* 180, 50–63.
- Oliveira, D.S., Xavier, D.S.F., Farias, P.N., Bezerra, V.S., Pinto, C.H.C., Souza, L.D., Santos, A.G.D.S., de Oliveira Matias, L.G., 2012. Obtenção do biodiesel através da transesterificação do óleo de *Moringa oleifera* Lam. *Holos* 1.
- O'Donnell, S., Demshemino, I., Yahaya, M., Nwadike, I., Okoro, L., 2013. A review on the spectroscopic analyses of biodiesel. *Eur. Int. J. Sci. Technol.* 2 (7), 137–146.
- Pereira, F.S.G., Brito Neto, E.X., Wei, S., Galvão, C.C., Lima, V.F., Silva, V.L., Lima Filho, N.M., 2016a. Produção de biodiesel metílico com óleo purificado de *Moringa oleifera* Lamarck. *Revista Virtual de Química* 8 (3), 873–888.
- Pereira, F.S.G., Schuler, A.R.P., de Silva, A.M.R.B., Galvão, C.C., do Nascimento Pereira, R., de Lima Filho, N.M., da Silva, V.L., 2016b. Turbidity and acidity as monitoring parameters in the purification of *Moringa oleifera* oil for biodiesel production. *Am. Chem. Soc. J.* 16 (3), 1–9.
- Prabakar, D., Manimudi, V.T., Suvetha, S., Sampath, S., Mahapatra, D.M., Rajendran, K., Pugazhendi, A., 2018. Advanced biohydrogen production using pretreated industrial waste: outlook and prospects. *Renew. Sustain. Energy Rev.* 96, 306–324.
- Premi, M., Sharma, H.K., Sarkar, B.C., Singh, C., 2010. Kinetics of drumstick leaves (*Moringa oleifera*) during convective drying. *Afr. J. Plant Sci.* 4 (10), 391–400.
- Rabelo, S.N., Ferraz, V.P., Oliveira, L.S., Franca, A.S., 2015. FTIR analysis for quantification of fatty acid methyl esters in biodiesel produced by microwave-assisted transesterification. *Int. J. Environ. Sustain. Dev.* 6 (12), 964–969.
- Rashid, U., Anwar, F., Moser, B.R., Knothe, G., 2008. *Moringa oleifera* oil: a possible source of biodiesel. *Bioresour. Technol.* 99 (17), 8175–8179.
- Ruttarattanamongkol, K., Siebenhandl-Ehn, S., Schreiner, M., Petrasch, A.M., 2014. Pilot-scale supercritical carbon dioxide extraction, physico-chemical properties and profile characterization of *Moringa oleifera* seed oil in comparison with conventional extraction methods. *Ind. Crops Prod.* 58, 68–77.
- Saravanan, A.P., Mathimani, T., Deviram, G., Rajendran, K., Pugazhendhi, A., 2018. Biofuel policy in India: a review of policy barriers in sustainable marketing of biofuel. *J. Clean. Prod.* 193, 734–747.
- Sawaya, W.N., Miski, A.M., Khalil, J.K., Khatchadourian, A.A., Mashadi, A.S., 1983. Physicochemical characterization of the major date varieties grown in Saudi Arabia. *Date Palm J.* 2, 1–25.
- Sayyar, S., Zainal Abidin, Z., Yunus, R., Muhammad, A., 2009. Extraction of oil from *Jatropha* seeds-optimization and kinetics. *Am. J. Appl. Sci.* 6 (7), 1390–1395.
- The American Oil Chemists' Society (AOCS), 2005. AOCS Standard Procedure Ba 6a-05. Crude Fiber in Feed by Filter Bag Technique. AOCS.
- Thiex, N., 2009. Evaluation of analytical methods for the determination of moisture, crude protein, crude fat, and crude fiber in distillers dried grains with solubles. *J. AOAC Int.* 92 (1), 61–73.
- Yang, L., Li, Y., Xg, G., Ma, X., Yan, Q., 2013. Comparison of dry ashing, wet ashing and microwave digestion for determination of trace elements in *Periostracum serpentinum* and *Periostracum cicadae* by icp-aes. *J. Chil. Chem. Soc.* 58 (3), 1876–1879.
- Yemmireddy, V.K., Chinnan, M.S., Kerr, W.L., Hung, Y.-C., 2013. Effect of drying method on drying time and physico-chemical properties of dried rabbiteye blueberries. *LWT - Food Sci. Technol. (Lebensmittel-Wissenschaft -Technol.)* 50 (2), 739–745.